Journal of Power Sources 213 (2012) 1–9

Contents lists available at SciVerse ScienceDirect

Journal of Power Sources

journal homepage: www.elsevier.com/locate/jpowsour

Enhancing proton conduction under low humidity by incorporating core–shell polymeric phosphonic acid submicrospheres into sulfonated poly(ether ether ketone) membrane

Lingli Nie [a], Jingtao Wang [a], Tao Xu [a], Hao Dong [a], Hong Wu [a,b], Zhongyi Jiang [a,*]

[a] Key Laboratory for Green Chemical Technology, School of Chemical Engineering and Technology, Tianjin University, Tianjin 300072, China
[b] Tianjin Key Laboratory of Membrane Science and Desalination Technology, Tianjin University, Tianjin 300072, China

ARTICLE INFO

Article history:
Received 25 December 2011
Received in revised form
30 March 2012
Accepted 31 March 2012
Available online 16 April 2012

Keywords:
Core–shell polymeric phosphonic acid submicrosphere
Sulfonated poly(ether ether ketone)
Water retention
Proton conduction
Direct methanol fuel cell membrane

ABSTRACT

Polymeric phosphonic acid submicrospheres (PPASs) with carboxylic acid cores and phosphonic acid shells are synthesized by distillation-precipitation polymerization. The structure and composition of PPASs are confirmed by transmission electron microscopy (TEM), Fourier transform infrared spectroscopy (FTIR), and energy dispersive X-ray (EDX). The PPASs are then incorporated into sulfonated poly(ether ether ketone) (SPEEK) to fabricate composite membranes for direct methanol fuel cells (DMFCs). The incorporated PPASs enlarge the ion-channel size of the composite membranes as testified by small-angle X-ray scattering (SAXS), affording significantly enhanced water uptake and water retention. Compared with the membrane containing the polymeric carboxylic acid submicrospheres (PCASs), the PPASs-filled membrane exhibits higher proton conductivity owing to the higher water uptake and water retention of the PPASs and stronger acidity of phosphonic acid. The composite membrane with 15 wt.% PPASs displays the highest proton conductivity of 0.0187 S cm^{-1} at room temperature and 100% relative humidity (RH). At the RH as low as 20%, this membrane acquires a proton conductivity of 0.0066 S cm^{-1}, 5 times higher than that of the SPEEK control membrane (0.0011 S cm^{-1}) after 90 min testing, at 40 °C.

1. Introduction

Conventional proton exchange membranes (PEMs), such as Nafion, having high proton conductivity under hydrated conditions are commonly utilized for direct methanol fuel cells (DMFCs). Water in PEMs plays a critical role in proton conduction by providing sufficient proton carriers and dissociating proton conducting groups [1]. Under the operating conditions of DMFCs, i.e. intermediate temperatures and low humidity, proton conductivity of most PEMs declines significantly due to the dehydration of membranes [2,3]. Therefore, improving water uptake and water retention of the PEMs remains to be a topic with great interest. One common approach is to incorporate hygroscopic inorganic fillers, such as zeolites [4], silica [5,6], and TiO_2 [7], which introduce numerous hydrogen-bond sites into the membranes. However, these inorganic fillers display low water uptake and rapid water release because of their weak interactions with water molecules [8]. Moreover, due to the low amount of proton conducting sites, the incorporation of inorganic fillers usually decreases proton conductivity of the resultant membranes [9,10]. Therefore, inorganic fillers are usually modified with proton conducting groups to solve these problems [11,12]. Thus, organic fillers rich in proton conducting groups might be better alternatives although scarcely reported in the literature. In our previous work, Wang et al. [13] dispersed polymeric carboxylic acid spheres into a sulfonated poly(ether ether ketone) (SPEEK) matrix, and found that the embedded fillers not only enhanced water retention property due to the functional groups with high water affinity, but also generated additional pathways for proton transport. Unfortunately, the relatively low proton conducting ability of –COOH groups on polymeric carboxylic acid spheres may restrict their wide application in PEMs. Therefore, polymeric spheres bearing both high water uptake and high proton conductivity are more desired.

The dominant proton conducting group in the majority of PEMs is sulfonic acid. However, phosphoric/phosphonic acids as protogenic groups have attracted increasing attention due to their high proton carrier concentration, thermal stability, and chemical stability [14]. Amphoteric phosphoric/phosphonic acids can serve as both proton donors and acceptors, accompanying with a high degree of self-dissociation even in anhydrous states. Additionally, phosphoric/phosphonic acid groups can form dynamical hydrogen-

* Corresponding author. Tel./fax: +86 022 23500086.
E-mail address: zhyjiang@tju.edu.cn (Z. Jiang).

0378-7753/$ – see front matter © 2012 Elsevier B.V. All rights reserved.
doi:10.1016/j.jpowsour.2012.03.108

bond networks, promoting a high mobility of proton carriers [14,15]. Therefore, the average zero point energy of phosphonic acids (37.2 kJ mol^{-1}) is much lower than that of sulfonic acids (69.9 kJ mol^{-1}), rendering a lower activation energy for proton hopping between phosphonic acid groups [16]. Besides, the binding energy with water of phosphonic acids (47.3 kJ mol^{-1}) is higher than that of sulfonic acids (44.4 kJ mol^{-1}), indicating a higher water retention property under low humidity conditions [16]. Thus, phosphoric/phosphonic acid functionalized materials are perceived as promising proton conduction promoters. One commonly utilized method is directly blending polymer membranes with phosphoric acids [17–22]. Nevertheless, the acid groups in the membranes are in free form and will be readily leached out by water or methanol molecules, which declines proton conduction. Another method is grafting phosphonic acid groups onto polymer main chains or side chains, so as to firmly immobilize the acid groups [23–29]. However, most of the grafting reactions are relatively complicated, and restricted by the harsh conditions and low reaction activities [30]. Therefore, it is still a great challenge to develop a method for immobilizing phosphonic acid groups in a well-controlled way, while avoiding a complicated procedure and harsh conditions.

In this study, polymeric phosphonic acid submicrospheres (PPASs) with carboxylic acid cores and phosphonic acid shells were designed and synthesized by distillation-precipitation polymerization, a facile and powerful technique for synthesizing monodisperse polymeric microspheres with different functional groups on their surfaces [31–33] and core–shell polymeric microspheres [34]. The PPASs were embedded into a SPEEK matrix for preparing composite membranes. The PPASs and the membranes were characterized by FTIR, EDX, TEM, FESEM, SAXS, and TGA. The effects of the incorporated PPASs on the membrane structure and performance, including morphology, nanophase separation, thermal stability, ion-exchange capacity (IEC), water uptake, water retention, methanol permeability and proton conductivity were investigated in detail.

2. Experimental

2.1. Materials and chemicals

Ethylene glycol dimethacrylate (EGDMA) and dimethyl vinylphosphonate (DMVP) were purchased from Alfa Aesar and utilized without further purification. 2, 2′-Azoisobutyronitrile (AIBN, analytical grade) and methacrylic acid (MAA, analytical grade) were purchased from Tianjin, and purified by vacuum distillation prior to utilization. Acetonitrile (analytical grade) was provided by Tianjin Chemical Reagents II Co. and dried over 4 Å molecular sieves and then distillated. Poly(ether ether ketone) particles (Victrex®PEEK, grade 381G) were supplied by Nanjing Yuanbang Engineering Plastics Co., Ltd. Dimethylformamide (DMF), sulfuric acid and methanol were of analytical grade and purchased locally. Deionized water was used throughout all experiments.

2.2. Synthesis of the polymeric carboxylic acid submicrospheres (PCASs) and PPASs

The PCASs with diameter of 270 nm were synthesized by distillation-precipitation polymerization according to the previous study [13]: EGDMA (1.60 mL, 1.68 g, 8.40 mmol), MAA (1.60 mL, 1.62 g, 18.63 mmol) and AIBN (0.06 g, 0.38 mmol, 2 wt.% relative to the comonomers) were dissolved in acetonitrile (80 mL) in a dried 100 mL flask, connected with a fractionating column, Liebig condenser, and a receiver. The mixture was heated from room temperature to the boiling state within 10 min and then the solvent was volatilized by distillation. After 1 h, the reaction was stopped and the resultant PCASs were purified by three cycles of centrifugation, decantation, and re-suspended in acetonitrile with ultrasonic-bathing. The PCASs were dried under vacuum at 50 °C until the weight did not change. The PPASs were synthesized by the same method: PCASs (0.30 g), DMVP (0.40 mL, 0.68 g, 5.00 mmol), EGDMA (0.60 mL, 0.63 g, 3.18 mmol) and AIBN (0.02 g, 0.13 mmol, 2 wt.% relative to the comonomers) were added into 80 mL acetonitrile. The same procedure was used for PPASs synthesis. The prepared polymeric phosphonate submicrospheres were dispersed into excess HCl aqueous solution (10 mol L^{-1}) at 100 °C for 24 h. Subsequently, the core–shell PPASs with diameter of 346 nm and shell thickness of about 38 nm were obtained. The resultant PPASs were dried in a vacuum oven at 50 °C till constant weight.

2.3. Preparation of SPEEK

PEEK was sulfonated according to the procedure in the literature [35]. PEEK (28 g) was dried at 60 °C for 24 h followed by being added slowly to concentrated sulfuric acid (H_2SO_4, 95–98 wt.%, 200 mL) under vigorous stirring at ambient temperature for 3 h and then at 45 °C for 8 h. The reaction was terminated by pouring the polymer solution into water under continuous agitation. The precipitated SPEEK was washed repeatly with de-ionized water until neutral pH and dried at ambient temperature for 24 h, and dried at 60 °C in a vacuum oven for another 24 h. The degree of sulfonation (DS) of SPEEK was 62% determined by titration.

2.4. Preparation of the membranes

The solution-casting method was adopted to prepare membranes. A certain amount of PCASs or PPASs were dispersed into 3 mL DMF under ultrasonic treatment and stirred for 12 h. 0.7 g SPEEK was added into 4 mL DMF later and stirred for 24 h. The submicrosphere-DMF was mixed with SPEEK-DMF solution under vigorous stirring at room temperature. The mixture was cast onto a glass plate and then dried under vacuum at 60 °C for 12 h, followed by further drying at 80 °C for another 12 h. After cooling down to room temperature, the membranes were peeled off from the glass plate. Then the membranes were immersed into 1.0 M HCl solution for 2 days and rinsed with de-ionized water to remove residual acid completely and dried in a vacuum oven at ambient temperature. The as-prepared membranes were designated respectively as SPEEK/PCASs-2.5, SPEEK/PCASs-5, SPEEK/PCASs-10, SPEEK/PCASs-15 or SPEEK/PPASs-2.5, SPEEK/PPASs-5, SPEEK/PPASs-10, SPEEK/PPASs-15, where 2.5, 5, 10, 15 were the weight percentage ratio of the submicrospheres to SPEEK. The SPEEK control membrane was prepared for comparison purpose and designated as SPEEK. All the membranes in our study were of thickness in the range of 70–80 μm.

2.5. Characterizations

The morphology of PCASs and PPASs was detected by transmission electron microscope (TEM, Tecnai G2 20 S-TWIN). Fourier transform infrared spectra (FTIR, 4000–400 cm^{-1}) of the submicrospheres and membranes were recorded on a Nicolet 6700 instrument. The content of phosphorus was measured by EDX using field emission scanning electron microscope (FESEM, Nanosem 430). The zeta-potential was determined with ZetaPALS (Brookhaven Instrument Cooperation) by measuring the electrophoretic mobility of the submicrospheres using de-ionized water as the electrolyte at room temperature. The cross-section of the membranes was characterized by FESEM after being freeze-fractured. The morphology of the membranes was determined by the small-angle X-ray scattering (SAXS) at a RigakuD/max2500v/Pc (CuK 40°kv, 200°mv) within the range of 0.20–5.00°. The thermal

stability of the samples was measured by thermogravimetric analysis (TGA) using a TGA-50 SHIMADZU. The samples were analyzed from 30 to 750 °C with a heating rate of 10 °C min^{-1} under nitrogen atmosphere.

2.6. Water uptake and water release

Prior to measurement, the submicrospheres and the membranes were dried in an oven at 60 °C for 24 h and then their dry weights (W_{dry}, g) were measured. The dried samples were soaked in de-ionized water at room temperature for 24 h. The surface water on the membranes was removed and then the membranes were immediately weighed to obtain their wet weights (W_{wet}, g). This procedure was repeated three times to gain the average water uptake with an error within ±5.0% and calculated by Eq. (1) respectively:

$$\text{Water uptake}(\%) = \frac{W_{wet} - W_{dry}}{W_{dry}} \times 100 \quad (1)$$

After measuring water uptake, the hydrated samples were stabilized in a constant temperature humidity chamber. The samples were weighed ($W_{wet.t}$, g) at the time of t at 40 °C and 20% RH. Water release as a function of time was calculated by Eq. (2):

$$\text{Water release}(\%) = \frac{W_{wet} - W_{wet.t}}{W_{wet} - W_{dry}} \times 100 \quad (2)$$

Simultaneously, water retention was determined by Eq. (3):

$$\text{Water retention}(\%) = \frac{W_{wet.t} - W_{dry}}{W_{dry}} \times 100 \quad (3)$$

2.7. Methanol permeability

Methanol permeability of the membranes was measured using a glass diffusion cell technique at room temperature [36]. The membrane was hydrated in de-ionized water and then clamped tightly between two compartments. One compartment was filled with 2 M methanol solution (30.0 mL) and the other with same volume of de-ionized water. The solutions in the compartments were under magnetic stirring. Because of the methanol concentration difference between the two compartments, methanol flow occurred across the membrane. The methanol concentration in the receiving compartment was measured, as a function of time, using a gas chromatography (Agilent 6820) equipped with a thermal conductivity detector (TCD) and a DB624 column. Methanol permeability (P, cm^2 s^{-1}) was the average of three measurements with an error within ±5.0% and calculated from Eq. (4):

$$P = S\frac{V_B l}{AC_{A0}} \quad (4)$$

where S is the slope of the straight line of concentration versus time, V_B is the volume of the solution in the receiving compartment, l, A, and C_{Ao} are the membrane thickness, effective membrane area, and feed concentration, respectively. The measurements errors were within ±5.0%.

2.8. Ion-exchange capacity

IEC values of submicrospheres and the membranes were estimated by titration. The samples in acid form were immersed into 2 M NaCl solution for 24 h at room temperature to transform H^+ into Na^+. The dissociated H^+ ions in the solution were then titrated with 0.01 M NaOH solution using phenolphthalein as indicator. The titration was repeated three times and the IEC was calculated from Eq. (5):

$$\text{IEC}\left(\text{mmol g}^{-1}\right) = \frac{0.01 \times 1000 \times V_{NaOH}}{W_d} \quad (5)$$

where V_{NaOH} is the volume of NaOH solution consumed in the titration and W_d is the weight of the dried membrane. The measurements were carried out with an accuracy of 0.001 mmol g^{-1}.

2.9. Proton conductivity and selectivity

Proton conductivity (σ, S cm^{-1}) of the membranes was estimated in a two-point-probe conductivity cell by the AC impedance spectroscopy method in vertical direction, and the membranes were measured by using a frequency response meter (FRA, Compactstat, IVIUM Tech.) at a potential of 20 mV and an alternating current frequency from 1 to 10^6 Hz at 20 or 100% RH. Proton conductivity of the membranes was calculated using Eq. (6):

$$\sigma = \frac{l_0}{AR} \quad (6)$$

where l_0 and A are the thickness and the effective surface area of the membrane, respectively, and R is the membrane resistance obtained from the FRA.

The selectivity was defined as the ratio of proton conductivity to methanol permeability, which was used to identify the potential

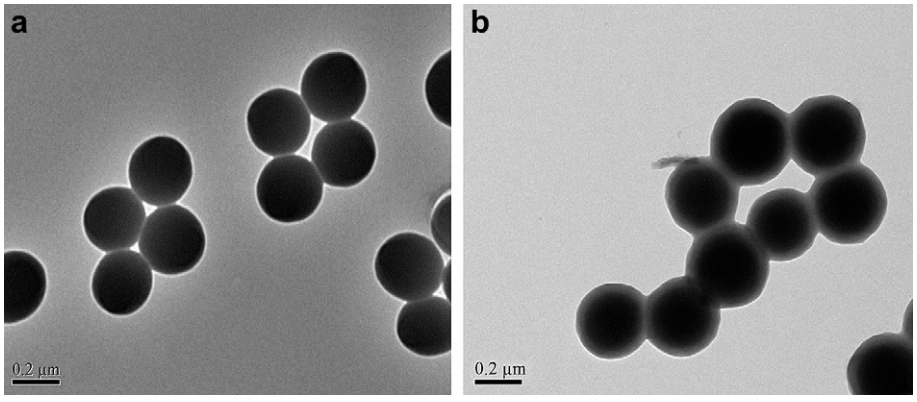

Fig. 1. TEM images of (a) PCASs, (b) PPASs.

membranes for DMFCs [37]. The selectivity could be obtained from Eq. (7):

$$S = \sigma/P \quad (7)$$

where S is the selectivity, and σ and P are proton conductivity and methanol permeability, respectively.

3. Results and discussion

3.1. Characterization of the submicrospheres

The TEM image in Fig. 1b demonstrated that the PPASs exhibited obvious core–shell structure with carboxylic acid cores of 270 nm and phosphonic acid shells of approximately 38 nm. PCASs with diameter of 270 nm without phosphonic acid shells were prepared for comparison purpose, as shown in Fig. 1a.

The chemical composition of the as-prepared submicrospheres was confirmed by FTIR and EDX in Fig. 2. The absorption peaks at 1730 and 1469 cm^{-1} for the PCASs were assigned to the stretching vibration of C=O and the bending of COO–H, respectively. Compared with the PCASs, the formation of phosphonic acid shells were confirmed by the P–O bending vibration (520 cm^{-1}) and O–H stretching vibration of the $-PO_3H_2$ (2610 and 2300 cm^{-1}), respectively. In addition, the asymmetric O–P–O stretching vibration (970 cm^{-1}) and the P=O stretching vibration (1240–1140 cm^{-1}) were overlapped by the C–OH stretching vibration of the PCASs [38]. EDX result in Fig. 2b and Table 1 revealed that the content of phosphorus was 1.57 At.% or 3.26 wt.%. The calculated $-PO_3H_2$ content was 8.52 wt.%, accordingly. Zeta potential value (Table 1) of the PPASs was higher (−54.38 mV) than that of the PCASs (−36.93 mV) at neutral conditions, implying that there were more electronegative charges on the PPASs surface. IEC values revealed that the PPASs had higher proton conduction ability than the PCASs (0.108 mmol g^{-1} for PPASs and 0.087 mmol g^{-1} for PCASs). TGA curves in Fig. 2c showed that the PPASs displayed a gradual weight loss from 150 °C owing to the reversible desorption of water produced by self-condensation of the phosphonic acid groups [27]. A large degradation step at around 340 °C resulted from the irreversible cleavage of the C–P bonds [23,29]. For the PCASs, initial weight loss began at 150 °C due to the adsorbed water and the carboxylic acid groups began to decompose at around 380 °C.

3.2. Characterization of the composite membranes

The cross-section morphology of the membranes as probed by FESEM (Fig. 3a–f) revealed that all the membranes were relatively dense, uniform and defect-free. The submicrospheres were homogeneously dispersed without obvious agglomeration within the SPEEK matrix. That was owing to electrostatic repulsive force between the phosphonic acid or carboxylic acid groups during collision of the submicrospheres in the membrane casting solution [39], as testified by zeta potential analysis.

FTIR (Fig. 4) spectra displayed the characteristic peaks at around 1221, 1078, and 1020 cm^{-1} for all the SPEEK membranes, which were assigned to the symmetric and asymmetric O=S=O stretching vibration of sulfonic acid groups, demonstrating the successful sulfonation of SPEEK [40]. Compared with the SPEEK control membrane (Fig. 4a), a new peak around 1720 cm^{-1} appeared for the composite membranes due to the C=O stretching vibration of the submicrospheres.

TGA of the membranes as shown in Fig. 5 indicated that all the membranes exhibited three distinct weight loss steps [41]. The first weight loss (from 150 to 240 °C) was ascribed to water evaporation

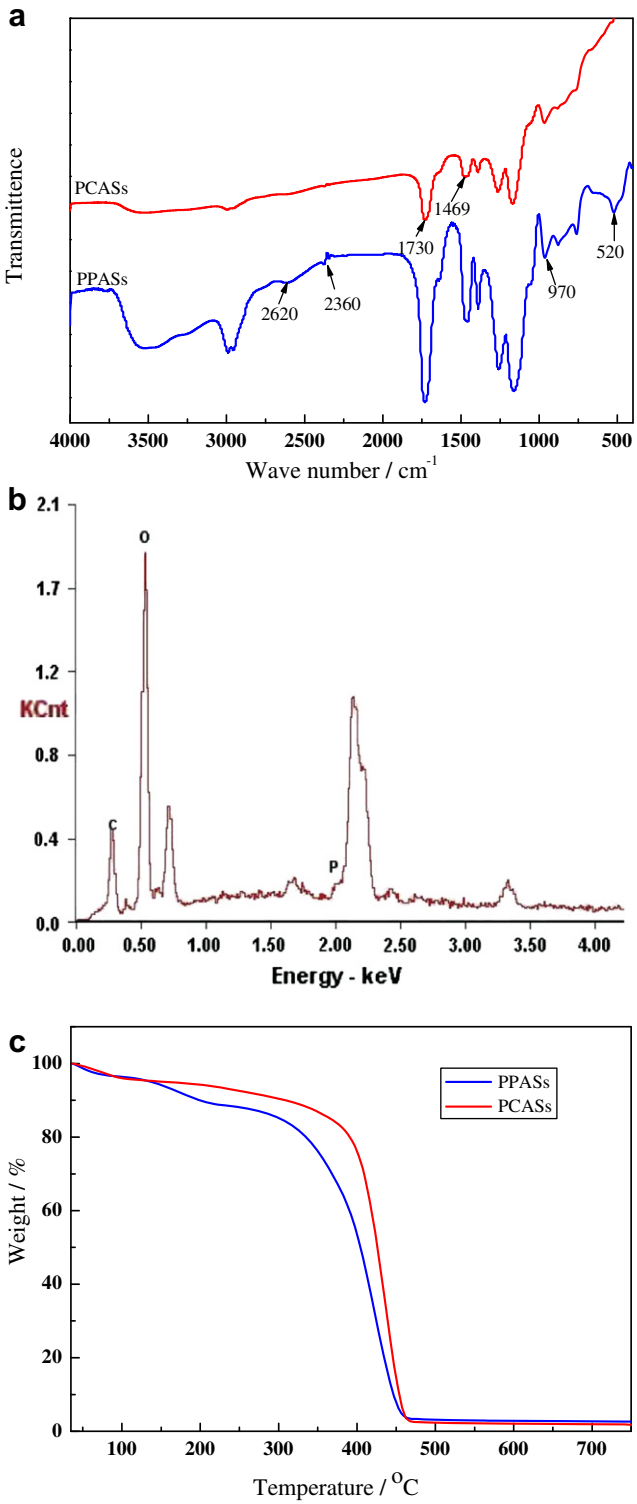

Fig. 2. (a) FTIR spectra of submicrospheres, (b) EDX of PPASs and (c) TGA of submicrospheres.

(free and bound water) of the membranes. The second weight loss step ranging from 240 to 370 °C was assigned to the degradation of the sulfonic acid groups. The final weight loss, beginning at 400 °C, was related to the decomposition of the polymer chains. It could be deduced that the weight loss of the composite membranes was similar to that of the SPEEK control membrane below 400 °C but

Table 1
Shell thickness, P content, zeta potential, *IEC* and water uptake of the submicrospheres.

Entry	Submicrosphere	Shell thickness (nm)	P content		Zeta potential (mV)	*IEC* (mmol g^{-1})	Water uptake (%)[a]
			(wt.%)	(At.%)			
1	PCASs	0	0	0	−36.93	0.087	98.95
2	PPASs	38 ± 2	3.26	1.57	−54.38	0.108	263.2

[a] Water uptake at 20 °C.

higher than that of the SPEEK control membrane above 400 °C. The char yield of the SPEEK control membrane and SPEEK/PCASs-10 were 46.58 and 45.00%, respectively. With the PPASs content increase from 2.5 to 15 wt.%, the ultimate weight percentage of the composite membranes decreased from 46.91 to 42.82%. That was mainly originated from the lower char yield of the PPASs (2.61%, Fig. 2c) than that of the SPEEK control membrane. Overall, thermal stability of the as-prepared membranes should be high enough (>240 °C) to meet the requirement for DMFCs.

SPEEK displayed a nanophase separation due to the presence of the hydrophobic and hydrophilic domains. The nanophase separation provided continuous channels for mass transport and affected the performances of the membranes, in terms of water uptake, proton conductivity and methanol permeability [42,43]. SAXS profiles of the membranes were shown in Fig. 6. The scattered vectors (q) were 0.524 and 0.510 nm^{-1} for the SPEEK control membrane and the SPEEK/PCASs-10 membrane, respectively. In comparison, the SPEEK/PPASs-10 membrane exhibited lower q value (0.505 nm^{-1}). Bragg spacing d, referring to the "center to center distance" between two clusters, can be calculated according to the equation $d = 2\pi/q$ [44]. Accordingly, the SPEEK/PPASs composite membranes possessed higher ion-channel size, indicating that the embedded submicrospheres disturbed the ordered structure of the ionic domains and this effect became more notable with the increase of submicrosphere content.

3.3. Water uptake, water release and water retention

Water uptake of the prepared membranes played a crucial role in proton conduction [45,46]. Water uptake of the SPEEK control membrane was 27.62% (Table 2). With the PPASs content increasing from 2.5 to 15 wt.%, water uptake of the composite membranes gradually increased from 33.39 to 39.68% (Table 2). The increased water uptake was mainly attributed to the incorporation of PPASs with high water storage ability (263.2%, Table 1) and enlarged ion-channel size of the SPEEK bulk, as testified by SAXS. Furthermore, the SPEEK/PCASs membranes exhibited higher water uptake over the SPEEK control membrane. Meanwhile, the PPASs-filled membranes possessed higher water uptake than the PCASs-filled membranes under identical conditions.

Reducing water loss would yield high proton conductivity at intermediate temperatures and low RH. The dynamic water release of PPASs and PCASs at 40 °C and 20% RH was shown in Fig. 7a, linear water release with time was observed in all the cases. The PPASs exhibited lower water release rate than the PCASs. This was probably due to the stronger interaction between phosphonic acid and

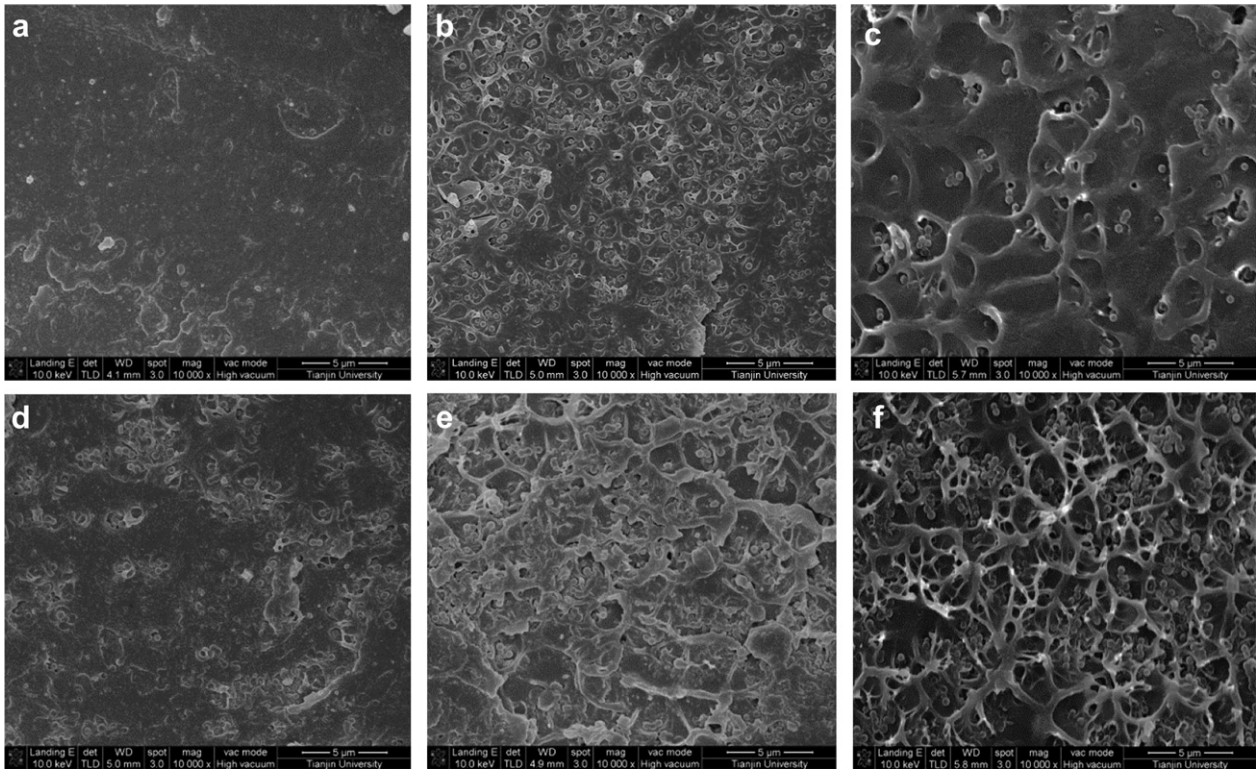

Fig. 3. FESEM images of the cross-section of (a) SPEEK, (b) SPEEK/PCASs-10, (c) SPEEK/PPASs-2.5, (d) SPEEK/PPASs-5, (e) SPEEK/PPASs-10, (f) SPEEK/PPASs-15.

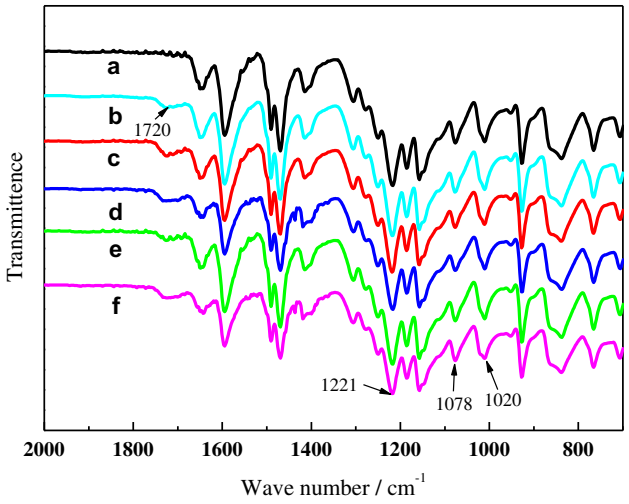

Fig. 4. FTIR spectra of (a) SPEEK, (b) SPEEK/PCASs-10, (c) SPEEK/PPASs-2.5, (d) SPEEK/PPASs-5, (e) SPEEK/PPASs-10, (f) SPEEK/PPASs-15.

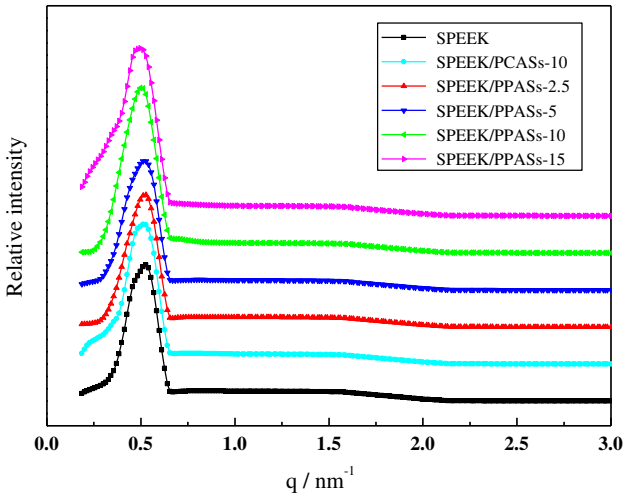

Fig. 6. SAXS curves of the membranes.

water molecule, which retained water molecule more tightly. The dynamic water release of the membranes displayed the similar trend as shown in Fig. 8a. Two stages could be observed clearly in water release curves: (i) in the first stage (0–70 min), water released sharply, which was mainly ascribed to the free water evaporation; and (ii) in the second stage (70–180 min), water lost slowly, mainly due to the bound water loss. For the SPEEK control membrane, water release was 93.52% after 180 min testing. Compared with the SPEEK control membrane, the PPASs-filled membranes showed lower water release rate. Especially as the PPASs content reached to 15 wt.%, the membrane displayed a water release as low as 73.94%.

Water retention of the submicrospheres and the membranes at 40 °C and 20% RH was presented in Fig. 7b and Fig. 8b, respectively, which revealed much higher water retention for the PPASs than the PCASs. For the PPASs-filled membranes, increasing water uptake and reducing water release rate endowed an increase of water retention (3.65–10.34%), when compared with that of the SPEEK control membranes (1.79%) after 180 min testing. Water retention of the SPEEK/PPASs membrane increased from 3.65 to 10.34% with the filler content in the range of 2.5–15 wt.%. Furthermore, the enhancing water retention of the PPASs conferred the SPEEK/PPASs membranes higher water retention compared with the SPEEK/PCASs membranes.

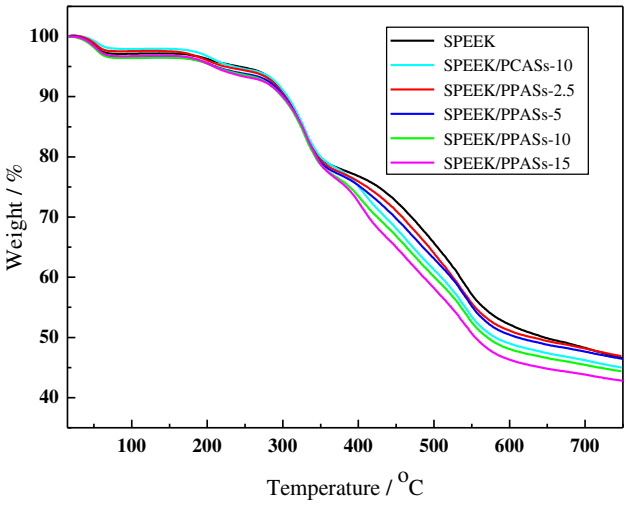

Fig. 5. TGA of the membranes.

3.4. IEC and proton conductivity

IEC was an important indicator of ionizable exchange hydrophilic groups in the samples. The IEC was measured by titration and presented in Table 2. IEC value of the SPEEK control membrane was 1.83 mmol g^{-1} and the DS was calculated to be 62%. With the incorporation of submicrospheres, IEC values of the composite membranes decreased, which was originated from the lower IEC values of the fillers than that of the SPEEK bulk. Consequently, with the PPASs content increase from 2.5 to 15 wt.%, IEC values of the SPEEK/PPASs membranes decreased from 1.69 to 1.52 mmol g^{-1}. The PPASs displayed higher IEC value than the PCASs, thus the SPEEK/PPASs membranes exhibited higher IEC values than the SPEEK/PCASs membranes under identical conditions.

Proton conductivity of the membranes at room temperature and 100% RH was summarized in Table 2. The SPEEK control membrane with 62% DS displayed a proton conductivity of 0.0069 S cm^{-1}, which was close to the literature results [47,48]. Compared with the SPEEK control membrane, the SPEEK/PPASs membranes displayed increased proton conductivity. Proton conductivity of the composite membranes increased from 0.0147 to 0.0187 S cm^{-1} as the PPASs content increased in the range of 2.5–15 wt.%. Such results were attributed to the presence of phosphonic acid groups and the increase of water content. The former rendered new proton carriers and proton could hop rapidly from one water molecule or group to another by forming and breaking dynamic hydrogen-bonds [15,38]. The latter facilitated proton transfer via vehicle mechanism by forming H_3O^+, $H_5O_2^+$, $H_7O_3^+$ and $H_9O_4^+$ [37,49]. Furthermore, the SPEEK/PPASs composite membranes exhibited higher proton conductivity than the SPEEK/PCASs composite membranes at the same filler content, consistent with IEC values and water uptake of the membranes. It is deserved to highlight that the addition of PPASs significantly increased proton conductivity of the SPEEK/PPASs membranes (0.0147–0.0187 S cm^{-1}) in comparison with the SPEEK control membrane (0.0069 S cm^{-1}). Although proton conductivity of the membrane was lower than that of Nafion 117 (0.048 S cm^{-1}) [50], it may be high enough to meet the requirement (>0.01 S cm^{-1}) for the DMFC membrane [51].

Proton conductivity at 40 °C and 20% RH as a function of time was shown in Fig. 9. For the SPEEK control membrane, proton

Table 2
Water uptake, *IEC*, methanol permeability, proton conductivity, and selectivity of the SPEEK control membrane and the composite membranes.

Entry	Membrane	Water uptake (%) [a]	*IEC* (mmol g^{-1})	Methanol permeability (10^{-7} cm^2 s^{-1})	Proton conductivity (S cm^{-1})[a]	Selectivity (10^5 S s cm^{-3})
1	SPEEK	27.62	1.83	2.14	0.0069	3.24
2	SPEEK/PCASs-2.5	28.12	1.67	2.40	0.0110	4.57
3	SPEEK/PCASs-5	29.87	1.59	2.47	0.0125	5.05
4	SPEEK/PCASs-10	30.77	1.53	2.32	0.0115	4.97
5	SPEEK/PCASs-15	31.16	1.49	2.47	0.0124	5.00
6	SPEEK/PPASs-2.5	33.39	1.69	2.38	0.0147	6.19
7	SPEEK/PPASs-5	34.53	1.60	2.42	0.0169	6.99
8	SPEEK/PPASs-10	37.87	1.54	2.28	0.0175	7.68
9	SPEEK/PPASs-15	39.68	1.52	2.38	0.0187	7.86

[a] The testing temperature is 20 °C.

conductivity sharply declined from 0.0069 to 0.0011 S cm^{-1}, reducing by 83.84% after 90 min testing. Such decline was mainly due to the serious water loss, which suppressed the dissociation degree of the sulfonic acid groups and disrupted the continuous ion-channels of the SPEEK bulk. Compared with the SPEEK control membrane, proton conductivity of the SPEEK/PPASs membranes only reduced by 74.46% (from 0.0147 to 0.0038 S cm^{-1}), 74.02% (from 0.0169 to 0.0044 S cm^{-1}), 72.61% (from 0.0175 to 0.0048 S cm^{-1}), 64.65% (from 0.0187 to 0.0066 S cm^{-1}), respectively, with 2.5, 5, 10 and 15 wt.% PPASs. The enhancement of proton conduction in the PPASs-filled membranes should be attributed to the increased water retention by incorporating the PPASs. Besides, the self-dissociation of phosphonic acid groups also facilitated proton conduction via Grotthus mechanism under low humidity. Furthermore, proton conductivity of the SPEEK/PCASs-10 membrane decreased more pronouncedly by 82.63% (from 0.0115

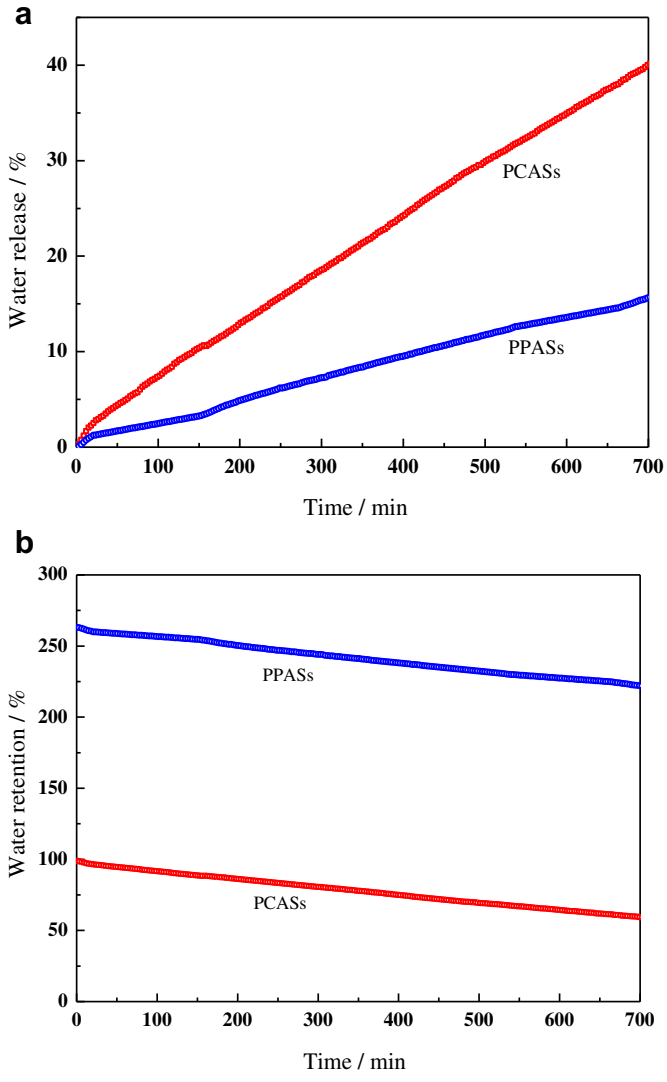

Fig. 7. The (a) Water release, (b) Water retention of the submicrospheres as a function of time at 40 °C and 20% RH.

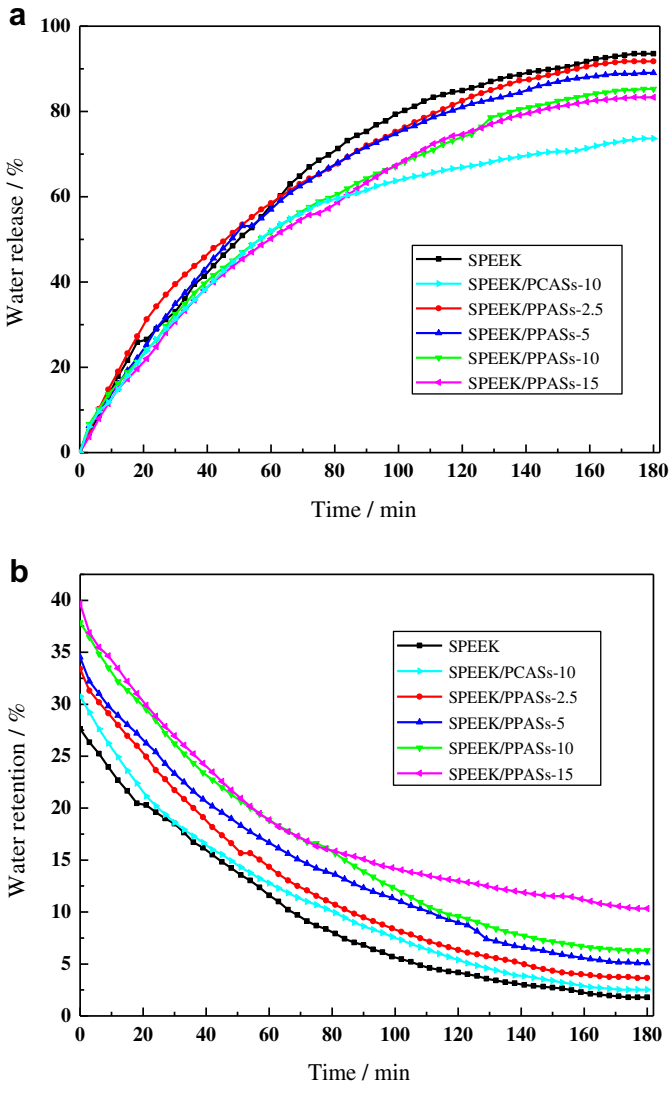

Fig. 8. The (a) Water release, (b) Water retention of the membranes as a function of time at 40 °C and 20% RH.

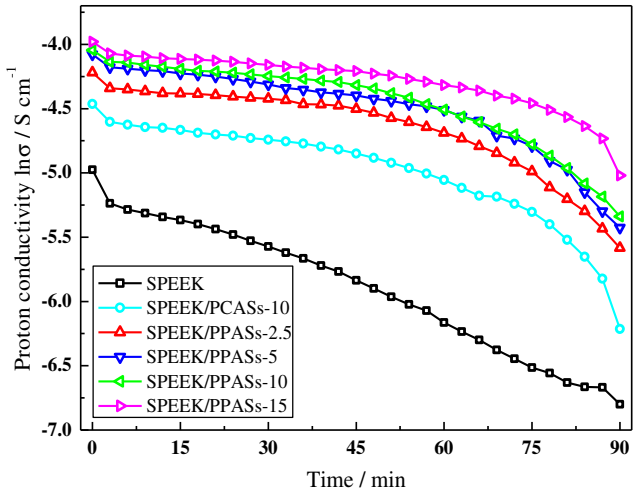

Fig. 9. Proton conductivity of the membranes as a function of time at 40 °C and 20% RH.

to 0.0020 S cm^{-1}) than that of the SPEEK/PPASs-10 membrane. The above results demonstrated that the SPEEK/PPASs composite membranes might be the competitive candidates for DMFC membranes under low humidity.

3.5. Methanol permeability and selectivity

Methanol permeability of the membranes was another key issue for PEMs, which was closely related to an open-circuit potential and fuel utilization efficiency [52]. As shown in Table 2, methanol permeability of the SPEEK control membrane was 2.14×10^{-7} cm^2 s^{-1}, which was much lower than that of Nafion 117 (3.14×10^{-6} cm^2 s^{-1}) [39]. The incorporation of PPASs induced two effects on methanol permeability: (i) the PPASs enlarged ion-channel size of the SPEEK bulk, which reduced the methanol diffusion resistance; and (ii) the high crosslink degree of PPASs prolonged the pathways of methanol transport, which increased the methanol barrier [53]. Due to these two reasons, the SPEEK/PPASs membranes exhibited a little higher methanol permeability than the SPEEK control membrane, and as the submicrosphere content increased, methanol permeability of the composite membranes changed only slightly.

Finally, selectivity was introduced to evaluate the comprehensive performance of the membranes (Table 2). Selectivity of the SPEEK control membrane was 3.24×10^5 S s cm^{-3}, while the composite membrane with 15 wt.% PPASs displayed 140% increase in selectivity (7.86×10^5 S s cm^{-3}).

4. Conclusion

In this study, core–shell PPASs were synthesized and embedded into a SPEEK matrix to prepare a series of composite membranes. The PPASs played dual roles in promoting proton conduction: (i) increasing water uptake and water retention, and enlarging ion-channel size of the membranes; and (ii) rendering new proton carriers and forming dynamic hydrogen-bond networks. The composite membrane with 15 wt.% PPASs displayed the highest proton conductivity (0.0187 S cm^{-1}) at room temperature and 100% RH. At the RH as low as 20%, this membrane acquired a proton conductivity of 0.0066 S cm^{-1}, 5 times higher than that of the SPEEK control membrane (0.0011 S cm^{-1}) after 90 min testing, at 40 °C. Moreover, the composite membrane containing 15 wt.% PPASs exhibited 140% increase in selectivity compared with the SPEEK control membrane. It was reasonable to conjecture that the SPEEK/PPASs-15 membrane could be a promising DMFC membrane candidate, in particular, under the application condition of low humidity.

Acknowledgments

We gratefully acknowledge financial support from National Science Fund for Distinguished Young Scholars (21125627), the Program of Introducing Talents of Discipline to Universities (B06006), and State Education Ministry and the National Basic Research Program of China through the ROCS Project (No.2008CB617502).

References

[1] K.D. Kreuer, S.J. Paddison, E. Spohr, M. Schuster, Chem. Rev. 104 (2004) 4637–4678.
[2] T.A. Zawodzinski, T.E. Springer, J. Davey, R. Jestel, C. Lopez, J. Valerio, S. Gottesfeld, J. Electrochem. Soc. 140 (1993) 1981–1985.
[3] T.A. Zawodzinski, M. Neeman, L.O. Sillerud, S. Cottesfeld, J. Phys. Chem. 95 (1991) 6040–6044.
[4] D.H. Son, R.K. Sharma, Y.G. Shul, H. Kim, J. Power Sources 165 (2007) 733–738.
[5] F. Pereira, K. Vallé, P. Belleville, A. Morin, S. Lambert, C. Sanchez, Chem. Mater. 20 (2008) 1710–1718.
[6] K.T. Adjemian, S. Srinivasan, J. Benziger, A.B. Bocarsly, J. Power Sources 109 (2002) 356–364.
[7] E. Chalkova, M.B. Pague, M.V. Fedkin, D.J. Wesolowski, S.N. Lvov, J. Electrochem. Soc. 152 (2005) A1035–A1040.
[8] H.M.L. Thijs, C.R. Becer, C. Guerrero-Sanchez, D. Fournier, R. Hoogenboom, U.S. Schubert, J. Mater. Chem. 17 (2007) 4864–4871.
[9] C.H. Rhee, Y. Kim, J.S. Lee, H.K. Kim, H. Chang, J. Power Sources 159 (2006) 1015–1024.
[10] Y. Kim, Y. Choi, H.K. Kim, J.S. Lee, J. Power Sources 195 (2010) 4653–4659.
[11] G. Alberti, M. Casciola, M. Pica, T. Tarpanelli, M. Sganappa, Fuel Cells 5 (2005) 366–374.
[12] G. Alberti, M. Casciola, E. D'Alessandro, M. Pica, J. Mater. Chem. 14 (2004) 1910–1914.
[13] J. Wang, S. Jiang, H. Zhang, W. Lv, X. Yang, Z. Jiang, J. Membr. Sci. 364 (2010) 253–262.
[14] M. Schuster, T. Rager, A. Noda, K.D. Kreuer, J. Maier, Fuel Cells 5 (2005) 355–365.
[15] H. Steininger, M. Schuster, K.D. Kreuer, A. Kaltbeitzel, B. Bingöl, W.H. Meyer, S. Schauff, G. Brunklaus, J. Maiera, H.W. Spiess, Phys. Chem. Chem. Phys. 9 (2007) 1764–1773.
[16] S.J. Paddison, K.D. Kreuer, J. Maier, Phys. Chem. Chem. Phys. 8 (2006) 4530–4542.
[17] J.S. Wainright, J.T. Wang, D. Weng, R.F. Savinell, M. Litt, J. Electrochem. Soc. 142 (1995) L121–L123.
[18] Y.-L. Ma, J.S. Wainright, M.H. Litt, R.F. Savinell, J. Electrochem. Soc. 151 (2004) A8–A16.
[19] C. Hasiotis, Q. Li, V. Deimede, J.K. Kallitsis, C.G. Kontoyannis, N.J. Bjerrum, J. Electrochem. Soc. 148 (2001) A513–A519.
[20] Y. Oono, A. Sounai, M. Hori, J. Power Sources 189 (2009) 943–949.
[21] A. Carollo, E. Quartarone, C. Tomasi, P. Mustarelli, F. Belotti, A. Magistris, F. Maestroni, M. Parachini, L. Garlaschelli, P.P. Righetti, J. Power Sources 160 (2006) 175–180.
[22] J.A. Asensio, S. Borrós, P. Gómez-Romeroa, J. Membr. Sci. 241 (2004) 89–93.
[23] J. Parvole, P. Jannasch, Macromolecules 41 (2008) 3893–3903.
[24] M. Ingratta, M. Elomaa, P. Jannasch, Polym. Chem. 1 (2010) 739–746.
[25] S.H. Kim, Y.C. Park, G.H. Jung, C.G. Cho, Macromol. Res. 15 (2007) 587–594.
[26] H.R. Allcock, M.A. Hofmann, C.M. Ambler, R.V. Morford, Macromolecules 35 (2002) 3484–3489.
[27] R. Perrin, M. Elomaa, P. Jannasch, Macromolecules 42 (2009) 5146–5154.
[28] B. Lafitte, P. Jannasch, J. Polym. Sci. Part A: Polym. Chem. 45 (2007) 269–283.
[29] J. Parvole, P. Jannasch, J. Mater. Chem. 18 (2008) 5547–5556.
[30] A.L. Rusanov, P.V. Kostoglodov, M.J.M. Abadie, V.Y. Voytekunas, D.Y. Likhachev, Adv. Polym. Sci. 216 (2008) 125–155.
[31] F. Bai, X. Yang, W. Huang, Macromolecules 37 (2004) 9746–9752.
[32] F. Bai, X. Yang, R. Li, B. Huang, W. Huang, Polymer 47 (2006) 5775–5784.
[33] S.F. Li, X.L. Yang, W.Q. Huang, Chin. J. Polym. Sci. 23 (2005) 197–202.
[34] D. Qi, F. Bai, X. Yang, W. Huang, Eur. Polym. J. 41 (2005) 2320–2328.
[35] L. Li, J. Zhang, Y. Wang, J. Membr. Sci. 226 (2003) 159–167.
[36] H. Wu, B. Zheng, X. Zheng, J.T. Wang, W.K. Yuan, Z.Y. Jiang, J. Power Sources 173 (2007) 842–852.
[37] B.S. Pivovar, Y. Wang, E.L. Cussler, J. Membr. Sci. 154 (1999) 155–162.
[38] Y. Jin, S. Qiao, J.C. Diniz da Costa, B.J. Wood, B.P. Ladewig, G.Q. Lu, Adv. Funct. Mater. 17 (2007) 3304–3311.
[39] J. Wang, H. Zhang, Z. Jiang, X. Yang, L. Xiao, J. Power Sources 188 (2009) 64–74.
[40] S. Zhong, X. Cui, H. Cai, T. Fu, K. Shao, H. Na, J. Power Sources 168 (2007) 154–161.

[41] Y. Zhang, H. Zhang, Y. Zhai, X. Zhu, C. Bi, J. Power Sources 168 (2007) 323–329.
[42] D.X. Luu, E.B. Cho, O.H. Han, D. Kim, J. Phys. Chem. B 113 (2009) 10072–10076.
[43] J. Won, H.H. Park, Y.J. Kim, S.W. Choi, H.Y. Ha, H. I-Oh, H.S. Kim, Y.S. Kang, K.J. Ihn, Macromolecules 36 (2003) 3228–3234.
[44] C. Zhao, H. Lin, K. Shao, X. Li, H. Ni, Z. Wang, H. Na, J. Power Sources 162 (2006) 1003–1009.
[45] J. Wang, H. Zhang, X. Yang, S. Jiang, W. Lv, Z. Jiang, S.Z. Qiao, Adv. Funct. Mater. 21 (2011) 971–978.
[46] C. Bi, H. Zhang, Y. Zhang, X. Zhu, Y. Ma, H. Dai, S. Xiao, J. Power Sources 184 (2008) 197–203.
[47] S. Xue, G. Yin, Eur. Polym. J. 42 (2006) 776–785.
[48] K.N.T. Do, D. Kim, J. Power Sources 185 (2008) 63–69.
[49] S. Feng, Y. Shang, G. Liu, W. Dong, X. Xie, J. Xu, V.K. Mathur, J. Power Sources 195 (2010) 6450–6458.
[50] H. Wang, B.A. Holmberg, L. Huang, Z. Wang, A. Mitra, J.M. Norbeck, Y. Yan, J. Mater. Chem. 12 (2002) 834–837.
[51] V. Neburchilov, J. Martin, H. Wang, J. Zhang, J. Power Sources 169 (2007) 221–238.
[52] A.F. Ismail, N.H. Othman, A. Mustafa, J. Membr. Sci. 329 (2009) 18–29.
[53] T. Fu, Z. Cui, S. Zhong, Y. Shi, C. Zhao, G. Zhang, K. Shao, H. Na, W. Xing, J. Power Sources 185 (2008) 32–39.